Influence of the Structural Period in the Input Energy Power

C. Frau(✉), S. Panella, and G. Gioacchini

Universidad Tecnológica Nacional, Regional Mendoza, Argentina
cdfrau@frm.utn.edu.ar

Abstract. Performance-Based Seismic Engineering requires the evaluation of ground motion intensity measures. This is also necessary for Energy-Based Design methodology which effect of ground motions on structures is considered as an energy input to structures. It is known that intensity measures of ground motion based on energy allow an improved characterization of different types of time histories. This is because energy is a cumulative measure of ground shaking and it captures the duration effects, frequency content and amplitude. In particular, the time that the ground motions deliver the energy is a relevant aspect that differs from the traditional acceleration response spectra which represents only the maximum response. To take in count the time in which the energy enters in the structure, and should be dissipated, previous works have introduced the power concept; it is defined as the total input energy divided by the time energy takes to enter to the structure. In the definition of the time to calculate the power the effective duration of the acceleration time history was used as the time interval between the 5% and 95% of the Arias Intensity. In this work the time interval in which the energy enter to the structure is studied. The time to calculate the power is obtained from the graph of input energy for each structural period. Thus, the parameters named as Input Energy Power, Input Energy Power Spectrum and Input Energy Power Intensity are redefined from this new definition of time. It was found that the time which the energy enters to the structure changes significative from a period to another, especially in near-fault record. When this time is compared with the structural period it is observed that in some cases the structures should dissipate a great amount of energy in a few strain cycles.

Keywords: Energy-Based Design · Input Energy Power · Influence of the structural period

1 Introduction

Seismic design requires a suitable evaluation of ground motion intensity; the definition of reliable design earthquakes, adequately representative of the destructive potential of the ground motion expected in a site, is the basic step in earthquake-resisting design of structures. Many studies have been carried out to evaluate the predictive capability of intensity measures (IMs) in literature, and effort for understanding how to improve these IMs has been made. Usually, the intensity of ground shaking and the demand on structures

A. A. Dindar et al. (Eds.): IWEBSE 2025, LNCE 692, pp. 1–13, 2025.
https://doi.org/10.1007/978-3-031-97129-7_8

have been characterized using parameters such as peak ground acceleration (PGA) as well as strength (or displacement) by response spectrum ordinates (e.g. pseudo-spectral acceleration at the fundamental period).

Many studies have been carried out to evaluate the predictive capability of the IMs currently available in literature. Due to the larger number of hazard curves available for peak ground acceleration (PGA) and spectral acceleration at the fundamental period of the structure, these two parameters are in general the most widely used as intensity measures.

Researchers have proposed other parameters to measure the ground motion intensity such as Arias Intensity (Arias, 1970), cumulative absolute velocity (CAV), Housner Intensity (IH) (Housner, 1952), Earthquake Destructiveness Power (PD) (Araya and Saragoni, 1980).

In recent years, some other IMs including spectrum intensity measures have been investigated and proved having better predictive abilities than PGA and Sa(T1) especially in the case of medium-period frame structures (Yakut and Yilmaz, 2008). Vector intensity measures have also been proposed (e.g., by Baker and Cornell, 2005; Luco et al., 2005) by adding to Sa(T1) other parameters for improving the correlations with respect to the predicted EDPs.

Methods based on the estimation of input energy and other energy parameters have also been proving effective in order to facilitate the determination of such design earthquakes, as the allow to characterize properly the different sorts of time histories (Decanini and Mollaioli, 2001). Several studies have advised the use of energy concepts as an alternative way to the traditional design strategies for the identification of the seismic demands imposed by the earthquakes (Zahrat and Hall, 1984; Uang and Bertero, 1990; Fajfar et al., 1990).

Damage and energy demand are closely related; thus, evaluation of energy demands is important in seismic design for two reasons. For one, input energy demand spectra, which includes all energy components (recoverable strain, kinetic energy, damping energy and hysteretic energy), give a clear picture of the cumulative damage potential of ground motions, much more so than elastic acceleration response spectra. Secondly, hysteretic energy demand spectra, serves to provide the information necessary to modify the ductility capacities in accordance with appropriate cumulative damage models.

Energy-based methodologies have shown that are a suitable method to design earthquake-resistant structures and to characterize the different types of time histories of ground motions such as impulsive periodic, with long-duration pulses, etc. because it simultaneously considers the dynamic response of a structure (Mollaioli et al., 2006).

The use of input energy spectra permits a rational assessment of the energy absorption and dissipation mechanisms that can be effectively adopted to balance the energy imparted to the structure. Elastic and inelastic input energy spectra are regarded as the most important demand descriptors for the damage potential of the ground motions (Decanini et al., 2000).

Since energy is a cumulative measure of ground shaking, it also captures duration effects. In fact, it is well known that a certain amount of seismic damage ca be due not only by de maximum response such as force or lateral displacement, but also by inelastic excursions below the maximum response. Therefore, energy demand parameters can

be considered reliable tools to use in seismic hazard analysis, for selectin earthquake scenarios, and establishing design earthquakes for many types of engineering analyses (15–21. Mollaioli et al. COMPDYM 2019).

In recent works, the evaluation of the power of the input energy has been presented, defined as the total energy delivered divided by the time taken by the earthquake to deliver it. To do this, it is necessary to define the time in which the energy is delivered. Previous works used the time corresponding to the Arias intensity as a measure of time, that is, the time between 5% and 95% of the Arias intensity.

In this paper, we redefine the time to be used to calculate the power of the input energy. The new definition considers a particular time for each structural period and therefore the passage from the energy spectrum to the power spectrum is not a constant but is a function of the structural period. This variation is analyzed, and the input energy and the input power are compared for a set of records containing impulsive and vibratory records of large earthquakes. It is observed that there are cases where input energy has very high values but when distributed over a long time the power decreases significantly.

2 Input Energy

Given viscous damped SDOF system subjected to horizontal earthquake excitation the equation of motion can be written (Chopra, 1995):

$$m\ddot{u}_t + c\dot{u} + f_s = 0 \tag{1}$$

where m = mass, c = damping coefficient, f_s = restoring force (can be expressed as

$$\ddot{u}_t = \ddot{u} + \ddot{u}_g \tag{2}$$

$f_s = ku$ in elastic systems), u_t = total displacement of the mass, u = relative displacement of the mass respect to the ground and, u_g earthquake ground displacement. Replacing Eq. (2) in (1) equation may be rewritten as:

$$m\ddot{u} + c\dot{u} + f_s = -m\ddot{u}_g \tag{3}$$

Depending upon whether Eq. (1) or (2) is used to deliver the energy equation, different definitions of input energies may result (Uang and Bertero, 1990).

2.1 Absolute Input Energy

Integrating Eq. (1) whit respect to u, Absolute Input Energy is obtained as follows:

$$\int m\ddot{u}_t du + \int c\dot{u} du + \int f_s du = 0 \tag{4}$$

Substituting $u = u_t - u_g$ and making a passage of terms yields

$$\int m\ddot{u}_t du_t + \int c\dot{u} du + \int f_s du = \int m\ddot{u}_t du_g \tag{5}$$

The right-hand-side term in the Eq. (5) is called Absolute Input Energy (Ei_a).
Substituting $du_g = \dot{u}_g dt$ yields

$$Ei_a/_m = \int_0^t \ddot{u}_t \dot{u}_g dt \tag{6}$$

2.2 Relative Input Energy

Integrating Eq. (3) whit respect to u, Relative Input Energy is obtained as follows:

$$\int m\ddot{u}du + \int c\dot{u}du + \int f_s du = -\int m\ddot{u}_g du \tag{7}$$

The right-hand-side term in the Eq. (7) is the Relative Input Energy (Ei_r). Substituting $du = \dot{u}dt$ yields

$$Ei_r/_m = \int_0^t \ddot{u}_g \dot{u} dt \tag{8}$$

In this work, Absolute Input Energy will be used. The reason is because it is more appropriate when the interest is on the seismic demand instead of the structural response. Absolute Input Energy represents the work made by the total base shear at the foundation on the foundation displacement (grown displacement).

3 Input Energy Power

Frau et al. (2023) and Frau and Panella (2024) introduced the concept of "Input Energy Power" (IEP). It was defined as the total input energy divided by the time energy takes to enter. Because the energy delivery is small at the beginning and the end of the seismic records to define IEP the effective duration was considered as the time interval between 5% and 95 of the Arias Intensity (Arias, 1970). After these works, new research has shown that the time energy takes to enter depends on the structural period. Thus, to consider this aspect a new definition of power is presented here. It considers a specific time to each structural system period.

3.1 Maximum Input Energy

For the definition of Input Energy Power (IEP), it is necessary to specify how is evaluated the Maximum Input Energy. In many cases, special in near-fault records, the Maximum Input Energy is not at the end of the record. To consider this aspect the peak of the input energy is considered although it is not at the end of the ground motion duration. Figure 1 a and b show two cases: one when the total input energy matches with the end of ground motion and another when the maximum input energy is before the end of ground motion. Although in this work elastic systems are analyzed, the idea of taking the peak in the time history of input energy can help to understand the collapse of structures when they must dissipate a lot of energy in a short time.

3.2 Effective Duration of Input Energy

According to how Maximum Input Energy is considered, Effective Duration (or effective time) is defined. For a particular structural period, the effective duration (t_{ef}) of input energy is defined as the time that elapses between 5% and 95% of the Maximum Input Energy. Figure 1 a and b show a case where Effective Duration takes a significative part

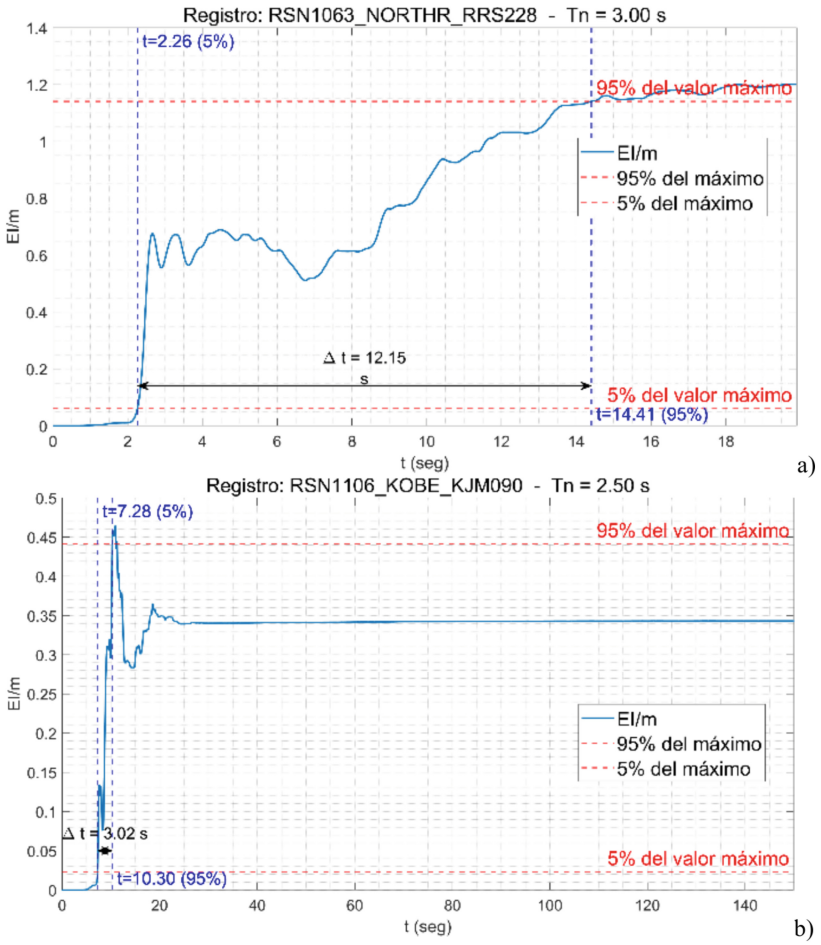

Fig. 1. Maximum Input Energy and effective duration; a) when the peak energy is at the end of the ground motion; b) when the peak energy is before the end of the ground motion.

of the ground motion, while the other, the Maximum Input Energy is delivered in a few seconds.

In Fig. 2 the effective duration for a ground motion is shown. In it can be seen large variations of the effective duration with the periods of the system. Effective duration is approximately 2 s for low periods and 20 s for periods near to 20 s; this is a ratio of 20. Figure 2 shows that the effective duration is very sensitive to the structural periods. Thus, a combination of maximum input energy and the time in which the energy is delivered is a better parameter to assess the severity of a ground motion, aspect occult in the input energy spectrum.

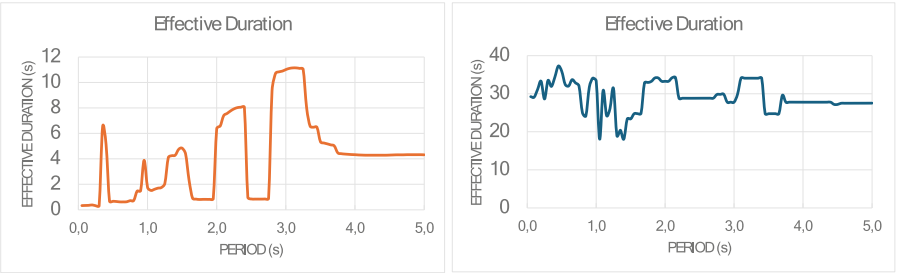

Fig. 2. Effective Duration (tef) vs structural period. Records #2 (Northridge) and #20 (Chile, 1985), (see Table 1).

If the effective duration (t_{ef}) is divided by the structural period (T_n) the number of cycles is obtained, it represents the number of oscillations that the structure does during the effective duration.

$$N°Cycles = t_{ef}(Tn)/Tn \tag{9}$$

Figure 3 shows the number of cycles for one of the cases studied. Can be seen that in a wide range of periods the number of cycles is less than 3, and in many cases, it takes values near to 1. Although these results are for elastic systems, it should be recognized that 90% of input energy must be dissipated in a few cycles. If the inelastic response were considered, it is known that the structural period is larger; this makes the situation more critical.

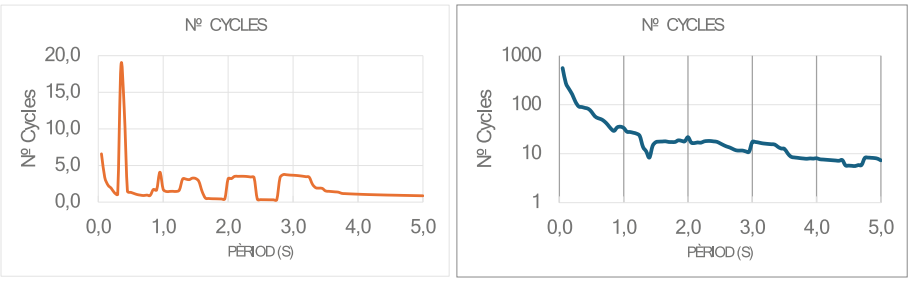

Fig. 3. Effective Duration and Nº of Cycles (tef/Tn). vs structural period. Records #2 (Northridge) and #20 (Chile, 1985), (see Table 1).

3.3 Input Energy Power

Given a SDOF system subjected to an earthquake grown motion, the Input Energy Power is defined as (Frau et al., 2023)

$$IEP(T_n, \xi) = \frac{Ei_a/m}{t_{ef}} \tag{10}$$

When this process is repeated for various SDOF systems with different periods for the same damping ratios, the Input Energy Power Spectrum is obtained (IEPS). This spectrum considers, in addition to the energy that enters, the time with which it does so, this is the energy in the unity time, the power. It should be recognized that the total amount of energy that enters is important, but also the time in which that energy must be dissipated, that is the power. Considering the effective duration for each structural period, the power spectrum captures for each structural period two essential aspects on destructivity or severity of a ground motion: the maximum energy that enters and the time which it do it. Figure 4 shows two cases studied; for period less to 2.0 s #11 ground motion has higher input energy than #7, but it presents lower input energy power; for periods greater 2.0 the situation is reversed.

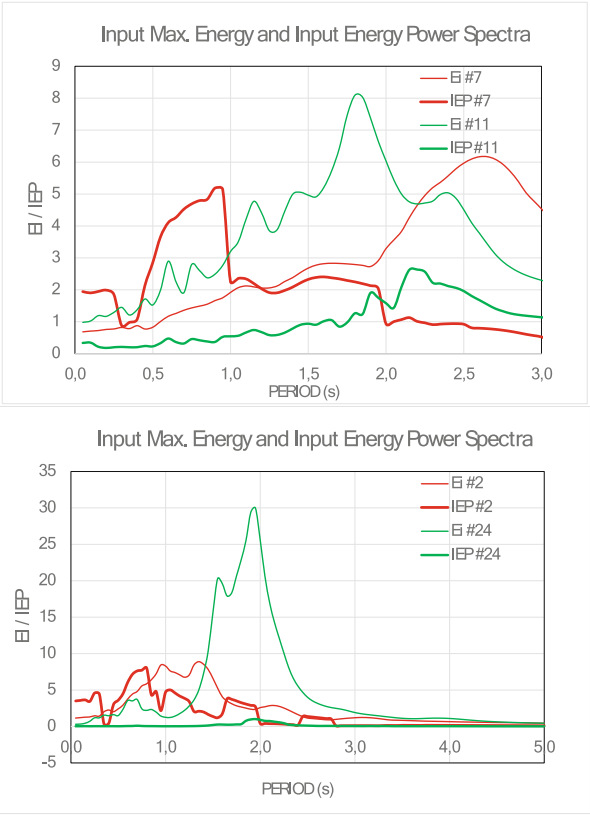

Fig. 4. Input Energy Spectrum vs Input Energy Power Spectrum. Records #7 vs 11 (top) and records #2 vs #24 (bottom)

With the same idea of Housner Intensity, the assessment of the Input Energy Power, a new parameter is defined: the Power Spectral Intensity (PSI). It is defined from the Input Energy Power Spectrum according to Eq. 11, it represents the area below the curve between 0.1 and 2.5 s (Frau et al., 2023, 2024). For comparative purposes and using the same criteria, we define Energy Spectral Intensity according to Eq. (12).

$$PSI = \int_{0.1}^{2.5} S_{IEP}(T, \xi) dT \tag{11}$$

$$ESI = \int_{0.1}^{2.5} S_{IE}(T, \xi) dT \tag{12}$$

4 Ground Motions Considered

For this study we selected a set of 29 ground motions. The seismic records used correspond to earthquakes from different parts of the world with a moment-magnitude between 6.5 and 9.0. They have very varied distances to the fault, from 1 km to more than 300 km. Records #1 to #15 can be considered near-fault; #16 to #19 belong to the Turkey earthquake (2023), a big shallow earthquake; in addition to them, we considered 4 subduction earthquakes: México (1985), Chile (1985 and 2010) and Japan (2011). Table 1 shows the main data of them.

Table 1. Ground motions considered in this study.

#	Earthquake	Country	Date	Station	Record Name	Magnitude	ClstD (km)
1	Northridge-01	EEUU	17/01/1994	Newhall - Fire Sta	RSN1044_NORTHR_NWH090	6,7	5,9
2	Northridge-01	EEUU	17/01/1994	Rinaldi Receiving Sta	RSN1063_NORTHR_RRS228	6,7	6,5
3	Kobe	Japan	16/01/1995	KJMA	RSN1106_KOBE_KJM090	6,9	1,0
4	Kocaeli	Turkey	17/08/1999	Yarimca	RSN1176_KOCAELI_YPT150	7,5	4,8
5	Chi-Chi	Taiwan	20/09/1999	CHY101	RSN1244_CHICHI_CHY101-N	7,6	9,9
6	Duzce	Turkey	12/11/1999	Bolu	RSN1602_DUZCE_BOL090	7,1	12,0
7	Denali	Alaska-EEUU	03/11/2002	TAPS Pump Station #10	RSN2114_DENALI_PS10-047	7,9	2,7
8	Darfield	New Zealand	03/09/2010	GDLC	RSN6906_DARFIELD_GDLCN55W	7,0	1,2
9	Darfield	New Zealand	03/09/2010	GDLC	RSN6906_DARFIELD_GDLCS35W	7,0	1,2
10	Darfield	New Zealand	03/09/2010	LINC	RSN6927_DARFIELD_LINCN23E	7,0	7,1
11	Superstition Hills-02	EEUU	24/11/1987	Parachute Test Site	RSN723_SUPERB_B-PTS225	6,5	1,0
12	Superstition Hills-02	EEUU	24/11/1987	Parachute Test Site	RSN723_SUPERB_B-PTS315	6,5	1,0
13	Loma Prieta	EEUU	18/10/1989	Gilroy Array #2	RSN766_LOMAP_G02090	6,9	11,1
14	El Mayor-Cucapah	Mexico	04/04/2010	El Centro Array #12	RSN8161_SIERRAMEX_E12090	7,2	11,3
15	El Mayor-Cucapah	Mexico	04/04/2010	El Centro Array #12	RSN8161_SIERRAMEX_E12360	7,2	11,3
16	Gaziantep	Turkey	06/02/2023	3129	20230206011732_3129_mp_RawAcc_E	7,7	75,7
17	Gaziantep	Turkey	06/02/2023	3129	20230206011732_3129_mp_RawAcc_N	7,7	75,7
18	Ekinözü	Turkey	06/02/2023	4612	20230206102447_4612_mp_RawAcc_E	7,6	62,2
19	Ekinözü	Turkey	06/02/2023	4612	20230206102447_4612_mp_RawAcc_N	7,6	62,2
20	Valparaíso (Algarrobo)	Chile	03/03/1985	Llolleo	CHILE1985.c.062w47LLa	7,8	37,9
21	Valparaíso (Algarrobo)	Chile	03/03/1985	Llolleo	CHILE1985.c.062w47LLc	7,8	37,9
22	Tōhoku	Japan	11/03/2011	Tsukidate - MYG004	MYG004 EW japon	9,0	75,1
23	Tōhoku	Japan	11/03/2011	Tsukidate - MYG004	MYG004 NS japon	9,0	75,1
24	El Maule	Chile	27/02/2010	Concepcion	concepcion1002271L	8,8	34,9
25	El Maule	Chile	27/02/2010	Concepcion	concepcion1002271T	8,8	34,9
26	Michoacán	Mexico	19/09/1985	SCT B-1	mex_SCT1_N00E	8,1	404
27	Michoacán	Mexico	19/09/1985	SCT B-1	mex_SCT1_N90E	8,1	404
28	Michoacán	Mexico	19/09/1985	UNAM	mex_CUMV_S00W	8,1	397
29	Michoacán	Mexico	19/09/1985	UNAM	mex_CUMV_S90W	8,1	397

5 Results

For each of the ground motions selected, the Input Energy Spectrum and the Input Energy Power Spectrum were calculated. From then, the follows parameters were obtained: a) Ei(máx), the peak of the Input Energy Spectrum; b) Tn (Ei_{max}), the period corresponding to Ei(max); c) IEP(Ei_{max}), the ordinate in the Input Energy Power Spectrum for Tn (Ei_{max}); d) IEP(max), is the peak of the Input Energy Power Spectrum and e) Tn(IEP_{max}), the period corresponding to IEP(max). Figure 5 shows these parameters. Table 2 shows the parameters described above for all the records selected. Effective duration was calculated too.

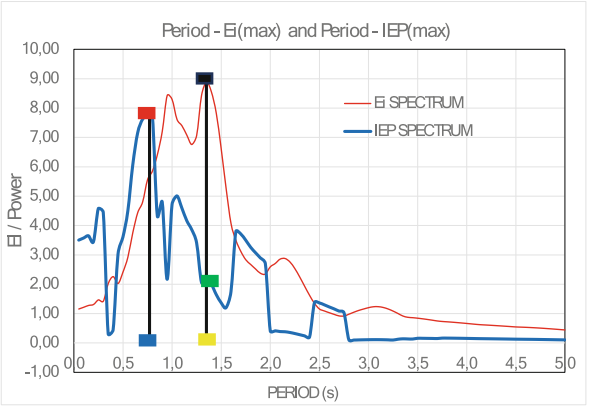

Fig. 5. Peak of the Input Energy Spectrum and Input Energy Power Spectrum and their corresponding periods. Ei(máx) (black); Tn (Ei_{max}) (yellow); IEP(Ei_{max}) (green); IEP(max) (red) and Tn(IEP_{max})(blue). Record #2.

When we look at the structural periods in which the peaks of the energy and power spectra occur, we see that these spectra do not always have their peaks at the same structural period. The records identified as near-fault present peaks at different periods, probably due to their impulsive characteristics. The vibratory type records contain frequencies in a narrow band and therefore the period corresponding to the peak of the energy spectrum coincides with the period corresponding to the power spectrum.

To compare the energy spectra with the power spectra, Fig. 6 is presented. The graph on the left compares Ei(máx), the peak of the Input Energy Spectrum with IEP(Ei_{max}), the ordinate in the Input Energy Power Spectrum for Tn(Ei_{max}). It is seen that some ground motions with relatively low input energy present the highest power input confirming that, in general, the highest power demand does not correspond to the highest energy demand; this situation is especially present in the records identified as near-fault. On the right of Fig. 6, the diagram shows the maximum ordinate of the Input Energy Spectrum Ei(max) with the maximum ordinate of the Input Power Spectrum IEP(max). In this case the effect described is significantly greater, confirming another relevant aspect which is that the highest energy and power demands are not found over the same structural period.

Table 2. Parameter of energy and power.

#	Earthquake	Tn (max Ei) (s)	t(efect.) (s)	Ei(máx) (m/s^2)	IEP(Eimáx) (m/s^2.s)	Tn(IEPmáx) (s)	t(efect.) (s)	IEP (max) (m/s2..s)	Nº Cycles Units
1	EEUU - Northridge	0,55	3,18	2,75	0,86	0,30	1,30	1,88	5,78
2	EEUU - Northridge	1,35	4,25	8,89	2,09	0,80	0,73	8,02	3,15
3	Japan - Kobe	0,70	5,56	6,15	1,11	0,75	1,16	4,70	7,94
4	Turkey - Kocaelli	3,50	15,60	4,00	0,26	1,40	5,30	0,45	4,46
5	Taiwan - Chi Chi	4,55	16,51	7,23	0,44	0,90	3,43	1,55	3,63
6	Turkey . Duzce	1,05	3,19	3,01	0,94	1,00	1,11	2,42	3,04
7	Alaske - Denali	2,65	7,86	6,17	0,79	0,90	0,32	5,19	2,96
8	New Zeland - Darfield	1,30	5,07	6,70	1,32	2,20	2,71	1,53	3,90
9	New Zeland - Darfield	1,40	4,82	7,61	1,58	1,30	2,72	1,97	3,44
10	New Zeland - Darfield	5,00	5,84	2,89	0,50	2,65	1,11	0,77	1,17
11	EEUU - Supert. 1987	1,80	6,40	8,09	1,26	2,20	1,78	2,63	3,56
12	EEUU - Supert. 1988	0,75	7,42	1,33	0,18	1,30	4,21	0,28	9,89
13	EEUU - Loma Prieta	1,45	4,81	2,46	0,51	1,25	2,15	0,64	3,32
14	México - El Mayor	1,10	15,77	2,60	0,17	1,05	6,12	0,31	14,3
15	México - El Mayor	0,95	4,30	2,28	0,53	0,95	4,30	0,53	4,52
16	Turkey - 2023	0,30	2,84	7,01	2,47	0,30	2,84	2,47	9,47
17	Turkey - 2023	1,15	3,39	11,07	3,26	1,00	1,18	6,01	2,95
18	Turkey - 2023	1,50	7,67	7,31	0,95	1,45	5,35	1,24	5,11
19	Turkey - 2023	1,45	6,60	16,06	2,43	1,20	0,54	7,09	4,55
20	Chile - Valpariso	0,40	34,47	3,20	0,09	0,40	34,47	0,09	86,2
21	Chile - Valpariso	0,50	31,86	6,90	0,22	0,55	24,57	0,23	63,7
22	Japan- 2011	0,20	70,28	10,82	0,15	0,20	70,28	0,15	351
23	Japan- 2011	0,20	74,19	47,62	0,66	0,25	40,18	0,66	371
24	Chile - Maule	1,95	30,06	29,97	1,00	1,95	30,06	1,00	15,4
25	Chile - Maule	1,55	58,54	18,66	0,32	1,65	24,97	0,60	37,8
26	Mexico -1985	2,01	27,69	12,05	0,43	2,05	27,69	0,43	13,8
27	Mexico -1985	2,05	24,57	21,87	0,89	2,05	24,57	0,89	12,0
28	Mexico -1985	2,00	21,32	0,33	0,02	2,00	21,32	0,02	11,0
29	Mexico -1985	2,00	31,22	0,11	0,00	2,15	9,69	0,01	5,00

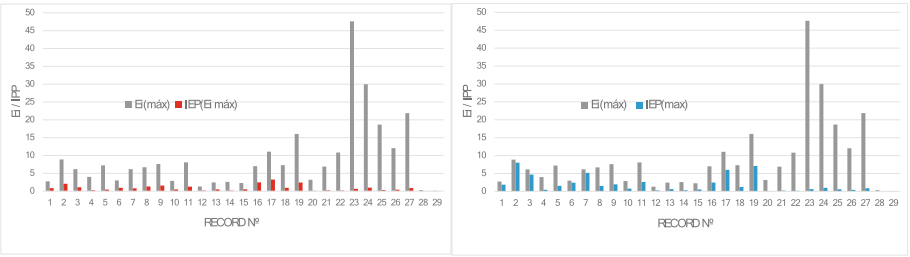

Fig. 6. Left: Ei(max) vs IEP(Ei_{max}). Right: Ei(max) vs IEP(max)

Figure 7 shows the effective time (or duration) for IEP(max) and the number of cycles equivalent to the effective time. In certain cases, the energy is delivered in a very short time (minor to 3 s) that involves a few cycles (3–6 cycles). It is a particular case record #10 taking just a little more than one cycle. On the other hand, records of large earthquakes take more than 10 cycles, with the special case of record #20 taking 86 cycles with an effective time of more than 30 s.

Now Power Spectral Intensity (PSI) and Energy Spectral Intensity are evaluated (Eq. 11 and 12); Table 3 shows these values for all ground motions studied. By integrating a band of structural periods (0.1–2.5 s) these parameters represent the intensity of the

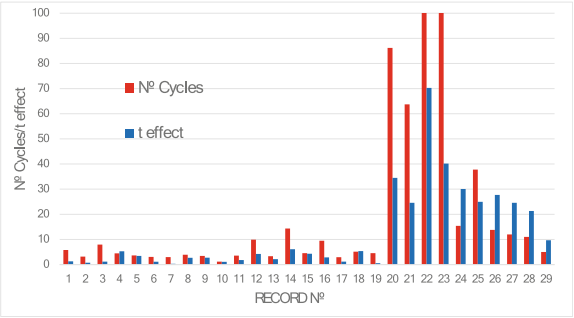

Fig. 7. Effective time and Nº Cycles for IEP(máx.)

ground motion with respect to the input energy. Thus, they allow us to identify records with high energy demands in short times for a wide frequency band.

Table 3. ESI and PSI, according to Eqs. 11 and 12.

#	Earthquake	Country	ESI (m/s)	PSI (m/s^2)
1	Northridge-01	EEUU	3,10	1,01
2	Northridge-01	EEUU	10,13	7,40
3	Kobe	Japan	4,57	1,63
4	Kocaeli	Turkey	2,09	0,38
5	Chi-Chi	Taiwan	5,18	0,96
6	Duzce	Turkey	3,20	1,37
7	Denali	Alaska-EEUU	6,08	5,63
8	Darfield	New Zealand	8,65	1,91
9	Darfield	New Zealand	8,65	2,39
10	Darfield	New Zealand	2,99	0,59
11	Superstition Hills-02	EEUU	9,80	2,30
12	Superstition Hills-02	EEUU	1,63	0,26
13	Loma Prieta	EEUU	1,83	0,74
14	El Mayor-Cucapah	Mexico	3,06	0,34
15	El Mayor-Cucapah	Mexico	2,50	0,25
16	Gaziantep	Turkey	6,41	0,93
17	Gaziantep	Turkey	15,16	6,27
18	Ekinözü	Turkey	5,95	0,94
19	Ekinözü	Turkey	10,77	5,74
20	Valparaíso	Chile	2,20	0,07
21	Valparaíso	Chile	4,94	0,18
22	Tōhoku	Japan	5,92	0,07
23	Tōhoku	Japan	10,91	0,15
24	El Maule	Chile	20,95	0,52
25	El Maule	Chile	10,56	0,19
26	Michoacán	Mexico	5,85	0,15
27	Michoacán	Mexico	10,80	0,42
28	Michoacán	Mexico	0,20	0,01
29	Michoacán	Mexico	0,11	0,01

To analyze the results obtained Fig. 8 has been prepared. In it, the Energy Spectral Intensity (ESI) has been ordered from lowest to highest for the 24 selected ground motions (blue bar chart). Corresponding to them, the Power Spectral Intensity (PSI) has been represented (red line). It can be observed that, in general, there is no correlation between the energy and power parameters; the red line does not follow the same trend as the blue bars. It is confirmed that certain records can have very high energy demands with very low power demands (e.g. # 17, 23, 24, 25, 27). Ground motions with high-energy intensity and high-power intensity would be the most destructive for a broadband frequency. Of the cases studied, records #2 (Northridge, USA), #7 (Alaska), #17 and #19 (Turkey) would be the most destructive.

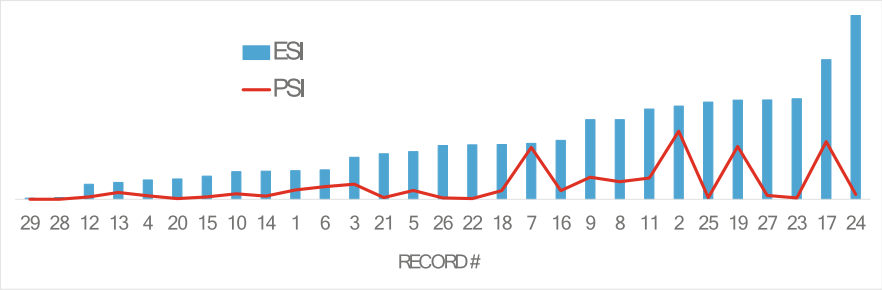

Fig. 8. ESI and PSI (ESI are sorted in order growing)

6 Conclusions

For this study a set of 29 ground motions was selected. They correspond to earthquakes from different parts of the world with varied distances to the fault. Set contains near-fault, big shallow earthquakes and subduction earthquakes.

To obtain the Input Energy Spectra and Input Energy Power Spectra, new criteria to determine the maximum input energy were proposed: one when the total input energy matches with the end of ground motion and another when the maximum input energy is before the end of ground motion. According to how Maximum Input Energy is considered, Effective Duration (or effective time) was defined as the time that elapses between 5% and 95% of the Maximum Input Energy. Dividing the effective duration (t_{ef}) by the structural period (T_n) the number of cycles ($N°_{Cy}$) to dissipate energy was obtained, it represents the number of oscillations that the structure does during the effective duration.

In general, the highest power demand does not correspond to the highest energy demand; in other words, the highest energy and power demands are not found over the same structural period. This situation is especially present in the records identified as near-fault.

The influence of the structural period is also present when the number of cycles corresponding to the effective duration are analyzed. Whitin a ground motion, a significant variation of the effective duration for the band of frequency analyzed was found; this affects directly in the number of cycles and the Input Energy Power in the spectrum.

Power Spectral Intensity (PSI) and Energy Spectral Intensity were evaluated. These parameters represent the intensity of the ground motion with respect to the input energy. PSI allows to identify records with high energy demands in short times for a wide frequency band. Ground motions with high-energy intensity and high-power intensity would be the most destructive for a broadband frequency.

Acknowledgements. The authors wish to express their gratitude to the Regional Center of Technological Development for Construction, Seismology and Earthquake Engineering (CeReDeTeC) of National Technological University (Argentina) for their support for the present study; to Fabrizio Mollaioli for his commentaries and Gabriel O. Becerra, civil engineering student at the Technological University for his collaboration in data processing.

AQ3

References

Araya, R., Saragoni, G.R.: Capacidad de los movimientos de producer daño estructural. Publicación SES 17/80 (in Spanish), División of Structural Engineering, Departament of Engineering. University of Chile (1980)

Arias, A.: A measure of earthquake intensity. In: Hansen, R. (ed.) Seismic design for nuclear power plants, pp. 438–483. MIT Press, Cambridge (1970)

Baker, J.W., Cornell, C.A.: A vector-valued ground motion intensity measure consisting of spectral acceleration and epsilon. Earthq. Eng. Struct. Dyn. **34**(10), 1193–1217 (2005)

Chopra, A.K.: Dynamics of Structures. Prentice Hall, Theory and Applications to Earthquake Engineering (1995)

Decanini, L.D., Mollaioli, F.: An energy-based methodology for assessment of seismic demand. Soil Dyn. Earthq. Eng. **21**, 113–137 (2001)

Decanini, L., Mollaioli, F., Saragoni, R.: Energy and displacement demands imposed by near-source ground motions. Proceedings of the 12th World Conference on Earthquake Engineering, New Zeland, paper 1136/6/A (2000)

Fajfar, P., Vidic, T., Fischinger, M.: Seismic demand in medium- and long-period structures. Earthquake Eng. Struct. Dynam. **18**(8), 1133–1144 (1989)

Frau, C.D., Panella, D.S., Tornello, M.E.: Input energy spectra for pulse-like ground motions. In: Varum, H., Benavent-Climent, A, Mollaioli, F. (eds.) Energy-Based Seismic Engineering. IWEBSE 2023. Lecture Notes in Civil Engineering, vol 236. Springer, Cham (2023). https://doi.org/10.1007/978-3-031-36562-1_17

Frau, C., Panella, S., Tornello, M.: Input energy power for near-fault and far-fault ground motions. Proceeding of the 18th World Conference on Earthquake Engineering, Milan, Italy, paper 5117 (2024)

Housner, G.W.: Intensity of ground motion during strong earthquakes. Earthquake Research Laboratory. California Institute of Technology (1952)

Luco, L., Manuel, L., Bazzurro, P.: Correlation fo damage of steel moment-resisting frames to a vector-valued ground motion parameter set that includes energy demands. Report prepared for USGS, Grant Nº 03HQGR0057 (2005)

Mollaioli, F., Bruno, S., Decanini, L., Panza, G.F.: Characterizaction of the dynamical response of structures to damaging pulse-type near-fault ground motions. Meccanica **41**, 23–46 (2006)

Mollaioli, F., Donaire-Avila, J.: Lucchini A and Benavent-Climent A. On the importance of Energy-Based parameters. COMPDYN. In: Papadrakais, M., Fragialdakis, M. (eds.) 7th ECCOMAS Thematic Conference on Computational Methods in Structural Dynamics and Earthquake Engineering. Crete, Greece (2019)

Uang, C.M., Bertero, V.V.: Evaluation of seismic energy in structures. Earthquake Eng. Struct. Dynam. **19**(1), 77–90 (1990)

Yakut, A., Yilmaz, H.: Correlation of deformation demands with parameter and characteristic period of near-fault ground motions. Earthq. Eng. Struct. Dyn. **38**(11), 1257–1280 (2009)

Zahrah, T.F., Hall, W.J.: Earthquake energy absorption in SDOF structures. J. Struct. Eng. **110**(8), 1757–1772 (1984)

Author Queries

Chapter 8

Query Refs.	Details Required	Author's response
AQ1	This is to inform you that corresponding author has been identified as per the information available in the Copyright form.	
AQ2	References 'Yakut and Yilmaz, 2008.' are cited in text but not provided in the reference list. Please provide references in the list or delete these citations.	
AQ3	References 'Yakut and Yilmaz (2009).' are given in list but not cited in text. Please cite in text or delete them from list.	

Alternative Texts for Your Images, Please Check and Correct them if Required

Page no	Fig/Photo	Thumbnail	Alt-text Description
5	Fig1	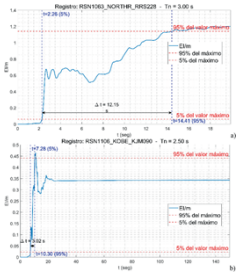	Two X-Y charts displaying seismic data. \\n\\nChart (a) shows "Registro: RSN1063_NORTHR_RRS228" with Tn = 3.00 s. The y-axis represents EI/m, and the x-axis represents time in seconds. Key points include t = 2.26 s at 5% and t = 14.41 s at 95%, with a time interval Δt = 12.15 s. Horizontal lines indicate 95% and 5% of the maximum value.\\n\\nChart (b) shows "Registro: RSN1106_KOBE_KJM090" with Tn = 2.50 s. The y-axis represents EI/m, and the x-axis represents time in seconds. Key points include t = 7.28 s at 5% and t = 10.30 s at 95%, with a time interval Δt = 3.02 s. Horizontal lines indicate 95% and 5% of the maximum value.\\n\\nBoth charts include legends and annotations in Spanish.
6	Fig2	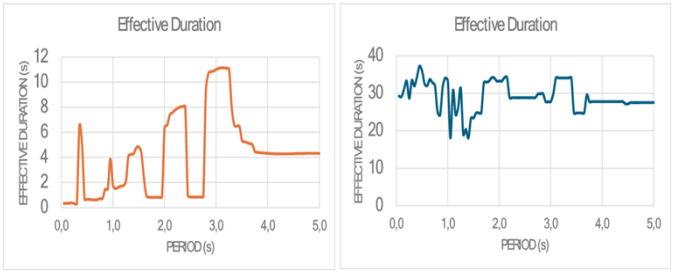	Two X-Y charts titled "Effective Duration" display data over a period in seconds. The left chart, in orange, shows fluctuating values between 0 and 12 seconds, peaking around 10 seconds. The right chart, in blue, depicts more stable values ranging from 20 to 40 seconds, with minor fluctuations. Both charts have "PERIOD (s)" on the x-axis and "EFFECTIVE DURATION (s)" on the y-axis.

Page no	Fig/Photo	Thumbnail	Alt-text Description
6	Fig3	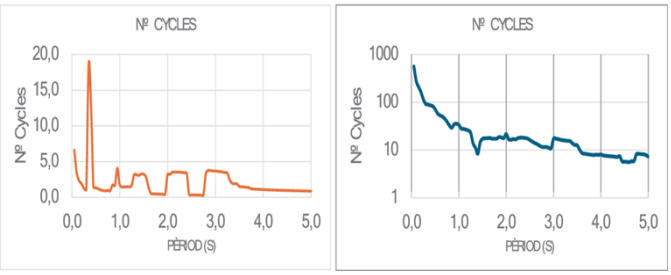	Two X-Y charts comparing the number of cycles against error values. The left chart, in red, shows a fluctuating pattern with peaks around 1.0 and 2.0 on the error axis, with cycles ranging from 0 to 20. The right chart, in blue, displays a decreasing trend on a logarithmic scale for cycles, ranging from 1 to 1000, with error values from 0 to 5. Both charts are titled "Nº CYCLES" and have the x-axis labeled as "ERROR (s)".
7	Fig4	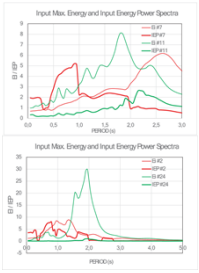	Two X-Y charts displaying "Input Max, Energy and Input Energy Power Spectra." The top chart shows data for BI #7, IEP #7, BI #11, and IEP #11, with the x-axis labeled "PERIOD (s)" ranging from 0 to 3.0, and the y-axis labeled "EI / EP" ranging from 0 to 9. The bottom chart presents data for BI #2, IEP #2, BI #24, and IEP #24, with the x-axis labeled "PERIOD (s)" ranging from 0 to 5.0, and the y-axis labeled "EI / EP" ranging from 0 to 35. Both charts use red and green lines to represent different data sets.
8	Tab1	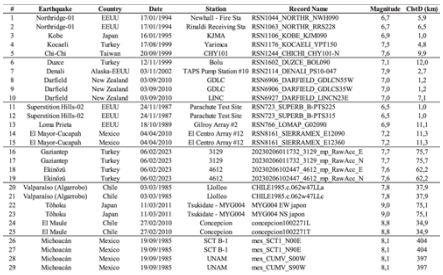	Table listing earthquake data, including columns for Earthquake name, Country, Date, Station, Record Name, Magnitude, and Cumulative Absolute Velocity (CAV) in cm/s. The table contains data for 26 earthquakes from various countries such as the USA, Japan, and Mexico, with magnitudes ranging from 6.2 to 8.1. Key entries include Northridge-01 in the USA with a magnitude of 6.7 and Kobe in Japan with a magnitude of 6.9.

Page no	Fig/Photo	Thumbnail	Alt-text Description
9	Fig5	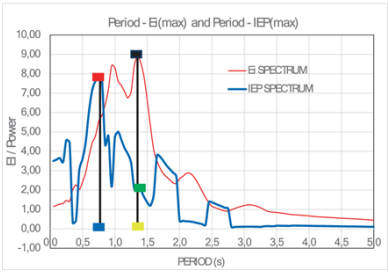	Chart showing two spectral lines labeled "B SPECTRUM" in red and "IBP SPECTRUM" in blue, plotted against the x-axis labeled "PERIOD (s)" and y-axis labeled "B / Power." The chart title is "Period - B(max) and Period - IER(max)." The red line peaks around 0.5 and 1.5 seconds, while the blue line follows a similar pattern with lower peaks. Colored markers highlight specific data points on the chart.
10	Tab2	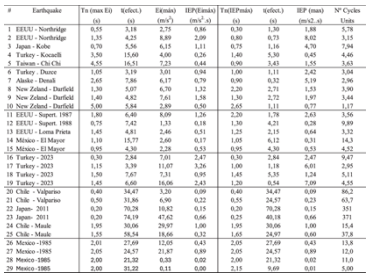	Table displaying seismic data for various earthquakes. Columns include earthquake number, name, Tn (max Ei) in seconds, t(effect.) in seconds, Ei(max) in m/s², IEP(Eimax) in m²/s²·s, Tn(IEPmax) in seconds, t(effect.) in seconds, IEP (max) in m²/s²·s, and number of cycles in units. Earthquakes listed include events from the USA, Japan, Turkey, Taiwan, Alaska, New Zealand, Mexico, Chile, and more, with data on maximum intensity, effective duration, and cycles.
10	Fig6	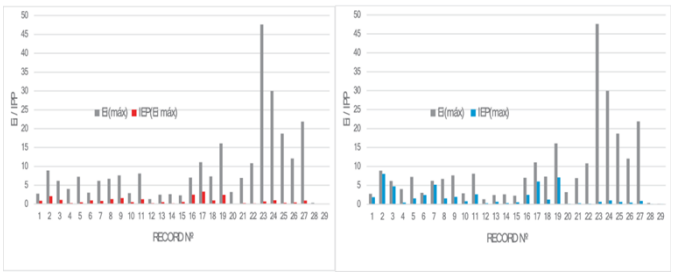	Two bar charts comparing data across 29 records. The left chart shows two data series: "E(max)" in gray and "ER(max)" in red. The right chart also displays "E(max)" in gray and "ER(max)" in blue. Both charts have the y-axis labeled as "E / IRP" with values ranging from 0 to 50, and the x-axis labeled as "Record No" from 1 to 29. The charts highlight variations in the data series across the records.

Page no	Fig/Photo	Thumbnail	Alt-text Description
11	Fig7	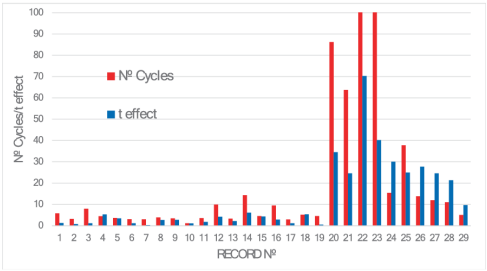	Bar chart showing the number of cycles and t effect across 29 records. The x-axis represents the record numbers, while the y-axis indicates the number of cycles or t effect. Red bars represent the number of cycles, and blue bars represent the t effect. Notable peaks occur between records 19 and 25, with the highest values around records 20 to 23.
11	Tab3		Table listing earthquakes with columns for earthquake number, country, ESI (m/s²), and PSI (m/s²). The table includes data for various locations such as the USA, Japan, Turkey, Taiwan, Chile, and Mexico. Each row provides specific ESI and PSI values for different earthquakes, indicating seismic intensity and peak ground acceleration.
12	Fig8		Bar and line chart showing data trends over records numbered 1 to 29. Blue bars represent ESI values, increasing steadily across records. A red line represents PSI values, showing periodic peaks and troughs. The chart highlights comparative trends between ESI and PSI.

#	Earthquake	Country	ESI (m/s)	PSI (m/s²)
1	Northridge-01	EEUU	3,10	1,01
2	Northridge-01	EEUU	10,13	7,40
3	Kobe	Japan	4,57	1,63
4	Kocaeli	Turkey	2,09	0,38
5	Chi-Chi	Taiwan	5,18	0,96
6	Duzce	Turkey	3,20	1,37
7	Denali	Alaska-EEUU	6,08	5,63
8	Darfield	New Zealand	8,65	1,91
9	Darfield	New Zealand	8,65	2,39
10	Darfield	New Zealand	2,99	0,59
11	Superstition Hills-02	EEUU	9,80	2,30
12	Superstition Hills-02	EEUU	1,63	0,26
13	Loma Prieta	EEUU	1,83	0,74
14	El Mayor-Cucapah	Mexico	3,06	0,34
15	El Mayor-Cucapah	Mexico	2,50	0,25

#	Earthquake	Country	ESI (m/s)	PSI (m/s²)
16	Gaziantep	Turkey	6,41	0,93
17	Gaziantep	Turkey	15,16	6,27
18	Ekinözü	Turkey	5,95	0,94
19	Ekinözü	Turkey	10,77	5,74
20	Valparaíso	Chile	2,20	0,07
21	Valparaíso	Chile	4,94	0,18
22	Tōhoku	Japan	5,92	0,07
23	Tōhoku	Japan	10,91	0,15
24	El Maule	Chile	20,95	0,52
25	El Maule	Chile	10,56	0,19
26	Michoacán	Mexico	5,85	0,15
27	Michoacán	Mexico	10,80	0,42
28	Michoacán	Mexico	0,20	0,01
29	Michoacán	Mexico	0,11	0,01